Electrothermal Instability in the Seeded Combustion Gas Boundary Layer near Cold Electrodes

Ken Okazaki,* Yasuo Mori,† Kunio Hijikata,‡ and Kazutomo Ohtake§
Tokyo Institute of Technology, Tokyo, Japan

A transition of discharge mode from diffuse to constricted or arc mode in the laminar boundary layer of the seeded combustion gas over a cold anode is analyzed by use of a linear stability theory on temperature and electrical fields. Cases of an externally applied electric field are investigated. For the basic steady distribution of unperturbed physical quantities in the boundary layer, an exact solution is used that is obtained as a result of analysis made around the anode by use of a three-fluid model. It is proven that when the parameter, expressed by the ratio of Joule heat to conductive heat of gas, exceeds a certain critical value, the diffuse mode discharge shows instability and that a transition of discharge mode to arc mode can occur as a result of electrothermal instability for small perturbations of gas temperature, electron temperature, current density, and electron number density. This type of instability is tightly connected with the extremely low electrical conductivity region near the cold electrode and the lower wall temperature brings about this instability more easily. It is also proven from a study for three kinds of surface boundary conditions of different physical situations that the instability is controlled by use of electrodes of higher thermal conductivity but lower electrical conductivity.

Nomenclature

C_p = specific heat at constant pressure
$\boldsymbol{E}$ = electric field vector
e = electron charge
h_p = Planck's constant
$\boldsymbol{J}$ = current density vector
J_0 = current density under the steady condition
k = Boltzmann's constant
m_e = electron mass
n = number density
P = pressure
Pr = Prandtl number
Q_{ex} = collision cross section for momentum exchange between electron and species X
q = amplification factor
Sc_i = Schmidt number of ion
T = gas temperature
T_e = electron temperature
t = time
$\boldsymbol{u}$ = mass average velocity vector [$\boldsymbol{u} = (u,v,w)$]
X = mole fraction
x,y,z = rectangular coordinates
α = wave number
α_e, α_X = recombination coefficients
δ = characteristic thickness of low electrical conductivity region
δ_x = electron energy loss factor of species X
ϵ = permittivity of free space
ϵ_i = ionization energy
λ = thermal conductivity
μ_e, μ_i = mobilities of electron and ion
ν = kinematic viscosity
$\bar{\nu}_{ex}$ = averaged collision frequency between electron and species X
ρ = mass density
σ = electrical conductivity

Subscripts

cr = critical value
e = electron
i = ion
K = potassium atom
s = Saha equilibrium value
w = wall or surface condition
X = species X, except ion and electron
∞ = main flow condition

Superscript

$\hat{(\ )}$ = nondimensional amplitude of perturbed quantity

Received Aug. 29, 1977; revision received Nov. 21, 1977.

Index categories: MHD; Plasma Dynamics and MHD.

*Graduate Student, Dept. of Physical Engineering.
†Professor, Dept. of Physical Engineering.
‡Associate Researcher, Dept. of Physical Engineering.
§Associate Professor, Dept. of Physical Engineering.

I. Introduction

In practical use of an open-cycle MHD power generation using a seeded combustion gas, the decrease of electrode lifetime caused by erosion due to local current concentration is one of the most serious problems to be solved. When electric current flows through the boundary layer of low electrical conductivity near the cold electrode, the discharge mode near the electrode changes with increasing current density.[1] When the current density is sufficiently small, the current flows almost uniformly into the electrode surface (diffuse mode), but when the current density becomes larger, many micro-arc spots are generated on the electrode surface where most of the current flows through these arcs of smaller cross sections (constricted mode). With further increase of current density, several arcs of large diameter (giant arcs) appear to carry most of the current. These arcs lead to excessive erosion of the electrode. The higher critical current density for this transition of discharge mode is expected for the hotter electrode. However, electrode materials of high thermal-shock resistance and anticorrosive properties have not been developed as yet for successfully long operation, but cold or semihot electrodes are currently considered to be the most promising candidates. Therefore, it will be very important to improve the electrode life by clarifying the physical process of transition from a diffuse discharge mode to a constricted arc mode near the cold electrode.

There have been many studies about arcs on electrodes of MHD generators,[2-7] but because of the complicated phenomena involved, some investigations have adopted rather unreasonable assumptions or conditions for their analyses. Dicks et al.[2] treat generation of arc spots by taking into consideration the interaction between the electrode

material and plasma in the extremely thin layer (about the Debye length) from the electrode surface. Hsu[4] and Oliver[5,6] discuss generation of current constriction in the plasma near the electrode by considering the energy balance for quantities perturbed from the diffuse mode. However, the quantities are assumed to be constant in the thickness proposed, which is ambiguously determined. Some have analyzed the condition for establishing current constriction mode, but few have discussed theoretically the generation of discharge instability. Oliver[6] states Hall effect to be one of the main causes in generating the instability, and Kon et al.[7] seemingly consider the effect of a magnetic field in a simplified model. But, in general, as the transition of discharge mode near the cold electrode could be characterized by the existence of a low-electrical-conductivity layer, most of the studies so far have investigated the case without a magnetic field.

Our present study discusses the problem theoretically by applying the linear stability theory with respect to small perturbations from the diffuse mode, on the assumption that generation of arc spots would result from transition of discharge mode from a uniform discharge to a constricted discharge due to electrothermal instabilities caused by an interaction of the temperature and electrical fields around the cold electrode. In a seeded combustion gas, when the electrode surface is cold and the current density is not too small, electron number density is reported not to be in Saha equilibrium for the gas temperature.[8] So, as a distribution of physical quantities under the steady condition in the boundary layer, an exact solution analyzed by use of a three-fluid model around the cold anode[8] is adopted. In this paper, the case of a laminar boundary layer over a flat-plate anode without a magnetic field is studied, and the case with a magnetic field will be reported elsewhere. An investigation of the critical condition of discharge stability is made by use of fundamental equations for perturbed fields, taking into account electron thermal and ionization nonequilibria, charge separation near the wall, and variation of physical properties of electrode materials.

II. Fundamental Equations and Boundary Conditions

A. General Equations

The field analyzed is shown in Fig. 1, together with the rectangular coordinate system, where x is the distance from the leading edge in the flow direction, y is the distance from the plate surface perpendicular to it, and the z axis is normal to the x and y axes. A laminar boundary layer is established on a cold flat-plate electrode, and it is assumed that there is a current flow by an external electric field between the main flow and the electrode. In the main flow, velocity, gas temperature, and pressure are assumed constant along the flow direction. The magnetic Reynolds number is sufficiently small and, for simplicity, density ρ, viscosity μ, thermal conductivity λ of the fluid, and electron and ion mobilities μ_e, μ_i are assumed constant. In this case, overall continuity and momentum equations are the conventional conservation equations in three dimensions. Other fundamental equations in the flow and electrical fields without magnetic field are described by use of a three-fluid model, taking charge separation into account as follows.[8]

Overall energy equation:

$$\frac{\partial T}{\partial t}+(u\cdot\nabla)T=\frac{\lambda}{\rho C_p}\nabla^2 T+\frac{1}{\rho C_p}J\cdot E \tag{1}$$

Fig. 1 Coordinate system.

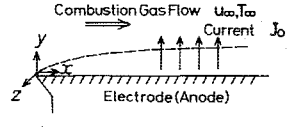

Electron continuity equation:

$$\frac{\partial n_e}{\partial t}+\frac{\partial}{\partial t}\left[\frac{\epsilon}{e}\nabla\cdot E\right]+(u\cdot\nabla)n_e+\nabla\cdot\left[\frac{\epsilon\mu_i}{e}(\nabla\cdot E)E-\frac{\nu}{Sc_i}\left(1+\frac{T_e}{T}\right)\nabla n_e\right]=\dot{n}_e \tag{2}$$

Electron energy equation:

$$\frac{\partial}{\partial t}\left[n_e\left(\frac{3}{2}kT_e+\epsilon_i\right)\right]+\sum_x \delta_x \bar{\nu}_{ex}\frac{3}{2}kn_e(T_e-T)=J\cdot E \tag{3}$$

Current conservation equation:

$$\nabla\cdot J=-\frac{\partial}{\partial t}(\epsilon\nabla\cdot E) \tag{4}$$

Maxwell's equation:

$$\nabla\times E=0 \tag{5}$$

Ohm's law:

$$J=\sigma E=en_e\mu_e E \tag{6}$$

In Eq. (3), because of the low electron number density, the fairly large electric field in the cold zone of the boundary layer near the electrode, and the extremely large electron energy loss factor associated with the electron/heavy-particle collision in the combustion gas, a dominant mechanism in the electron energy exchange is considered to be the local energy balance between the energy gained from the electric field and the energy loss by inelastic collisions with heavy particles. The terms including $\nabla\cdot E$ result from charge separation by using Poisson's equation. In Ohm's law [Eq. (6)], the contribution of the ion flux is neglected. The electron diffusion term is also neglected because it is made certain[8] that the electron diffusion flux is an order-of-magnitude smaller than the drift flux for $J=10\ \mathrm{A/m^2}$, and that the contribution of the electron diffusion flux gets much smaller for higher current densities. This simplified expression of Ohm's law is used only to give $\nabla\cdot E$ terms.

The bulk gas velocity, gas temperature, electron number density, and electron temperature for steady flow are obtained by solving the boundary-layer equations around the flat plate, and the following well-known transformation is adopted to simplify fundamental equations:

$$\xi=x,\qquad \eta=y\sqrt{u_\infty/2\nu x} \tag{7}$$

Local similarity is assumed to be a good approximation for the solution of the steady condition. For perturbation, if one assumes a standing plain wave solution with the wave number vector in the z direction, the forms of solutions of steady and perturbed components for fundamental equations just described can be expressed as

$$u=u_\infty[f'(\eta)+\hat{u}(\eta)f_u(\alpha z)g_u(\xi)\exp(qt)] \tag{8}$$

$$v=-\sqrt{u_\infty\nu/2\xi}\,[\{f(\eta)-\eta f'(\eta)\}+\hat{v}(\eta)f_v(\alpha z)g_v(\xi)\exp(qt)] \tag{9}$$

$$w=u_\infty[0+\hat{w}(\eta)f_w(\alpha z)g_w(\xi)\exp(qt)] \tag{10}$$

$$P=\rho u_\infty^2[p_0(\eta)+\hat{p}(\eta)f_p(\alpha z)g_p(\xi)\exp(qt)] \tag{11}$$

$$T=T_\infty[\theta(\eta)+\hat{t}(\eta)f_t(\alpha z)g_t(\xi)\exp(qt)] \tag{12}$$

$$T_e=T_\infty[\theta_e(\eta)+\hat{t}_e(\eta)f_e(\alpha z)g_e(\xi)\exp(qt)] \tag{13}$$

$$J_y = J_0[1 + \hat{j}_y(\eta) f_{jy}(\alpha z) g_{jy}(\xi) \exp(qt)] \tag{14}$$

$$J_z = J_0[0 + \hat{j}_z(\eta) f_{jz}(\alpha z) g_{jz}(\xi) \exp(qt)] \tag{15}$$

$$n_e = n_{e\infty}[\zeta(\eta) + \hat{n}_e(\eta) f_n(\alpha z) g_n(\xi) \exp(qt)] \tag{16}$$

Here, a prime ($'$) denotes differentiation with respect to η and q is assumed real. In each of the preceding equations, assuming the perturbation term is much smaller than the steady term and substituting Eqs. (8-16) into fundamental equations, the equations for the basic and steady unperturbed field are obtained as follows:

$$f''' + ff'' = 0 \tag{17}$$

$$(1/Pr)\theta'' + f\theta' = -H \tag{18}$$

$$G(1/\zeta^2) = (\sqrt{\theta_e}/\theta)(\theta_e - \theta) \tag{19}$$

$$f\zeta' + \frac{\partial}{\partial \eta}\left[A_1 \frac{1}{\zeta^3}\zeta' + A_2\left(1 + \frac{\theta_e}{\theta}\right)\zeta'\right] = -R \tag{20}$$

where

$$H = \frac{2\xi}{\rho u_\infty C_p T_\infty} \frac{J_0^2}{e\mu_e n_{e\infty}\zeta}$$

$$G = \frac{J_0^2}{2en_{e\infty}^2 \mu_e \rho u_\infty^2 p_0 \sqrt{\dfrac{8kT_\infty}{\pi m_e}} \displaystyle\sum_x \delta_x Q_{ex} X_x}$$

$$A_1 = \frac{\epsilon \mu_i J_0^2}{e^3 \mu_e^2 n_{e\infty}^3 p}, \quad A_2 = \frac{1}{Sc_i}, \quad R = \frac{2\xi[\dot{n}_e]_0}{n_{e\infty} u_\infty}$$

$$[\dot{n}_e]_0 = (\alpha_{e\infty}\zeta\theta_e^{-9/2} + \alpha_{x\infty}\theta^{-1}\theta_e^{-5/2}) n_{e\infty}^2(\zeta_s^2 - \zeta^2)$$

Here, α_e is a recombination coefficient, the third body of which is an electron, and α_x is a recombination coefficient, the third body of which is a heavy particle X.[8]

Because it is difficult to treat the beginning of discharge instability in a general manner, the following type of nearly two-dimensional original perturbations are considered in this analysis.

$$g_u,\ g_v,\ g_w,\ g_p,\ g_t,\ g_e,\ g_{jy},\ g_{jz},\ g_n = 1 \tag{21}$$

$$f_u,\ f_v,\ f_p,\ f_t,\ f_e,\ f_{jy},\ f_n = \sin\alpha z \tag{22}$$

$$f_w,\ f_{jz} = \cos\alpha z \tag{23}$$

The conditions of $q>0$ and $q<0$ correspond to unstable and stable conditions, respectively. The condition of $q=0$ corresponds to neutral stability and an analysis for the neutral stability is made in the following by putting $q=0$. Then, putting $\beta = 2\xi\alpha$, $\gamma^2 = (2\nu\xi/u_\infty)\alpha^2$, equations for the perturbed field are obtained as follows by linearizing the fundamental equations:

$$\eta\hat{u}' + \hat{v}' + \beta\hat{w} = 0 \tag{24}$$

$$\hat{u}'' + f\hat{u}' + (\eta f'' - \gamma^2)\hat{u} + f''\hat{v} + \eta\hat{p}' = 0 \tag{25}$$

$$\hat{p}' = 0 \tag{26}$$

$$\hat{w}'' + f\hat{w}' - \gamma^2\hat{w} - \beta\hat{p} = 0 \tag{27}$$

$$\hat{t}'' + Prf\hat{t}' - \gamma^2\hat{t} + Pr\eta\theta'\hat{u} + Pr\theta'\hat{v} + 2PrH\hat{j}_y - (PrH/\zeta)\hat{n}_e = 0 \tag{28}$$

$$\hat{n}_e'' - C_1\hat{u} - C_2\hat{v} + D_1\hat{n}_e' + D_2\hat{n}_e + D_3\hat{j}_y' + D_4\hat{j}_y + D_5\hat{t}' + D_6\hat{t} + D_7\hat{t}_e' + D_8\hat{t}_e = 0 \tag{29}$$

$$\hat{t}_e = F_1\hat{n}_e + F_2\hat{j}_y + F_3\hat{t} \tag{30}$$

$$\hat{j}_y' - \gamma\hat{j}_z = 0 \tag{31}$$

$$\hat{j}_y'' - (\zeta'/\zeta)\hat{j}_y' - \gamma^2\hat{j}_y = -(1/\zeta)\gamma^2\hat{n}_e \tag{32}$$

Equation (30) is written, in derivative form, as

$$\hat{t}_e' = F_1\hat{n}_e' + (F_4 - F_1F_7)\hat{n}_e + F_2\hat{j}_y' + (F_5 - F_2F_7)\hat{j}_y + F_3\hat{t}' + (F_6 - F_3F_7)\hat{t} \tag{33}$$

where

$$D_0 = -\frac{1}{\zeta^3}A_1 - \left(1 + \frac{\theta_e}{\theta}\right)A_2$$

$$D_1 = \left[\frac{6\zeta'}{\zeta^4}A_1 - \left(\frac{\theta_e'}{\theta} - \frac{\theta_e\theta'}{\theta^2}\right)A_2 - f\right]\Big/D_0$$

$$D_2 = \left[\left(\frac{3\zeta''}{\zeta^4} - \frac{12(\zeta')^2}{\zeta^5}\right)A_1 + \left(1 + \frac{\theta_e}{\theta}\right)A_2\gamma^2 + 2\zeta(\zeta\theta_e^{-9/2} + S\theta^{-1}\theta_e^{-5/2})B - (\zeta_s^2 - \zeta^2)\theta_e^{-9/2}B\right]\Big/D_0$$

$$D_3 = -(\zeta'/\zeta^3)A_1/D_0$$

$$D_4 = \left[\frac{6(\zeta')^2}{\zeta^4} - \frac{2\zeta''}{\zeta^3}\right]A_1/D_0$$

$$D_5 = (\zeta'\theta_e/\theta^2)A_2/D_0$$

$$D_6 = \left[\left(\frac{\zeta''\theta_e}{\theta^2} + \frac{\zeta'\theta_e'}{\theta^2} - \frac{2\zeta'\theta_e\theta'}{\theta^3}\right)A_2 + (\zeta_s^2 - \zeta^2)S\theta^{-2}\theta_e^{-5/2}B\right]\Big/D_0$$

$$D_7 = -(\zeta'/\theta)A_2/D_0$$

$$D_8 = \left[\left(\frac{\zeta'\theta'}{\theta^2} - \frac{\zeta''}{\theta}\right)A_2 - (\zeta\theta_e^{-9/2} + S\theta^{-1}\theta_e^{-5/2})\left(\frac{\partial \ln n_{es}}{\partial \ln T_e}\right)_0 \times \frac{2\zeta_s^2}{\theta_e}B + (\zeta_s^2 - \zeta^2)\left(\frac{9}{2}\zeta\theta_e^{-11/2} + \frac{5}{2}S\theta^{-1}\theta_e^{-7/2}\right)B\right]\Big/D_0$$

and

$$F_0 = (\zeta^2/2\sqrt{\theta_e})(3\theta_e - \theta), \quad F_1 = -2\zeta\sqrt{\theta_e}(\theta_e - \theta)/F_0$$

$$F_2 = 2G\theta/F_0, \quad F_3 = [G + \zeta^2\sqrt{\theta_e}]/F_0$$

$$F_4 = -[2\zeta'\sqrt{\theta_e}(\theta_e - \theta) + \frac{\zeta\theta_e'}{\sqrt{\theta_e}}(\theta_e - \theta) + 2\zeta\sqrt{\theta_e}(\theta_e' - \theta')]/F_0$$

$$F_5 = 2G\theta'/F_0, \quad F_6 = [2\zeta\zeta'\sqrt{\theta_e} + \zeta^2\theta_e'/2\sqrt{\theta_e}]/F_0$$

$$F_7 = \left[\frac{\zeta\zeta'}{\sqrt{\theta_e}}(3\theta_e - \theta) - \frac{\zeta^2\theta_e'}{4\theta_e^{3/2}}(3\theta_e - \theta) + \frac{\zeta^2}{2\sqrt{\theta_e}}(3\theta_e' - \theta')\right]\Big/F_0$$

$$C_1 = \eta\zeta'/D_0, \qquad C_2 = \zeta'/D_0$$

$$B = (2\xi n_{e\infty}/u_\infty)\alpha_{e\infty}, \quad S = \alpha_{x\infty}/\alpha_{e\infty}, \quad \zeta_s = n_{es}(T_e)/n_{e\infty}$$

The perturbation equations [Eqs. (24-32)] constitute a closed set of equations for nine unknown quantities ($\hat{u}$, $\hat{v}$, $\hat{w}$, $\hat{p}$, $\hat{t}$, $\hat{t}_e$, $\hat{j}_y$, $\hat{j}_z$, and $\hat{n}_e$). However, Eqs. (24-27) are not coupled to Eqs. (28-32) because of the no-magnetic-field assumption and are themselves closed. Therefore, when the set of Eqs.

(24-32) is regarded as making up an eigenvalue problem of the wave number and the ratio of Joule heat to conductive heat described below, Eqs. (24-27) cannot have any nontrivial solution and $\hat{u}$ and $\hat{v}$ should be taken to be zero. Then only the eigenvalue problems for Eqs. (28-32) has to be solved, letting $\hat{u}$ and $\hat{v}$ be zero. Thus, Eqs. (28-32) are rearranged as the following equations for $\hat{n}_e$, $\hat{j}_y$, and $\hat{t}$:

$$\hat{n}_e'' + W_1\hat{n}_e' + W_2\hat{n}_e + W_3\hat{j}_y' + W_4\hat{j}_y + W_5\hat{t}' + W_6\hat{t} = 0 \tag{34}$$

$$\hat{j}_y'' - (\zeta'/\zeta)\hat{j}_y' - \gamma^2\hat{j}_y + (1/\zeta)\gamma^2\hat{n}_e = 0 \tag{35}$$

$$\hat{t}'' + Pr f\hat{t}' - \gamma^2\hat{t} - (1/\zeta^2)h^2\hat{n}_e + (2/\zeta)h^2\hat{j}_y = 0 \tag{36}$$

where

$$W_1 = D_1 + D_7F_1, \quad W_2 = D_2 + D_7F_4 + D_8F_1 - D_7F_1F_7$$

$$W_3 = D_3 + D_7F_2, \quad W_4 = D_4 + D_7F_5 + D_8F_2 - D_7F_2F_7$$

$$W_5 = D_5 + D_7F_3, \quad W_6 = D_6 + D_7F_6 + D_8F_3 - D_7F_3F_7$$

and

$$h^2 = (2\nu\xi/u_\infty)(J_0^2/\lambda\sigma_\infty T_\infty) \tag{37}$$

$$\gamma^2 = (2\nu\xi/u_\infty)\alpha^2 \tag{38}$$

In Eq. (37), h^2 is a ratio of Joule heat to conductive heat in the gas, strongly related to the condition of discharge stability, and γ^2 is a nondimensional wave number.

B. Saha Equilibrium Case

In the case of the seeded combustion gas used as a working fluid, when the electrode surface temperature is low and the seed fraction is small, large electron thermal and ionization nonequilibria exist near the surface.[8] However, when the surface temperature is high and the seed fraction is large, the electron number density is appropriately given by Saha equilibrium value for the gas temperature, and equations for such a case can be obtained from Eqs. (34-36). This corresponds to the limiting case where both the inelastic electron energy loss factor and the electron-ion recombination coefficient are infinitely large. Arranging Eq. (34) with these conditions, perturbed electron number density is given by

$$\hat{n}_e = (\zeta/\theta)(\partial\ell n n_{es}/\partial\ell n T)_0\hat{t} \tag{39}$$

Substituting Eq. (39) into Eqs. (35) and (36), the following equations are obtained as fundamental equations for perturbations of gas temperature and current density:

$$\hat{t}'' + Pr f\hat{t}' - \left[\gamma^2 + \frac{h^2}{\zeta\theta}\left(\frac{\partial\ell n n_{es}}{\partial\ell n T}\right)_0\right]\hat{t} = -\frac{2h^2}{\zeta}\hat{j}_y \tag{40}$$

$$\hat{j}_y'' - \frac{\zeta'}{\zeta}\hat{j}_y' - \gamma^2\hat{j}_y = -\frac{1}{\theta}\left(\frac{\partial\ell n n_{es}}{\partial\ell n T}\right)_0\gamma^2\hat{t} \tag{41}$$

The Saha equilibrium equation, when electron thermal equilibrium is attained, is given by

$$n_e^2/(n_K - n_e) = 2\cdot(Z_{K^+}/Z_K)(2\pi m_e kT/h_p)^{3/2}\exp(-\epsilon i/kT) \tag{42}$$

where Z_{K^+} and Z_K are partition functions of potassium ion and atom. Therefore, for a weakly ionized gas of Saha equilibrium, the following equation is obtained.

$$(\partial\ell n n_{es}/\partial\ell n T)_0 = 3/4 + \epsilon_i/2kT \tag{43}$$

C. Thin Region Model

A more simplified model is considered. Since the discharge instability in the case of low-surface temperature is mainly influenced by the region of low electrical conductivity near the surface, considering δ as a characteristic thickness of the low electrical conductivity region in which physical quantities under steady unperturbed conditions are assumed constant, and neglecting the convection effect, Eqs. (40) and (41) are transformed into the following forms.

$$\hat{t}'' - (\gamma_*^2 + h_*^2)\hat{t} = -g\hat{j}_y \tag{44}$$

$$\hat{j}_y'' - \gamma_*^2\hat{j}_y = -(2h_*^2/g)\gamma_*^2\hat{t} \tag{45}$$

where $(')$ denotes differentiation with respect to $\eta_*(=y/\delta)$, and nondimensional parameters are

$$\gamma_*^2 = \delta^2\alpha^2$$

$$h_*^2 = (\delta^2 J_0^2/\lambda\sigma T)(\partial\ell n n_{es}/\partial\ell n T)_0$$

$$g = 2\delta^2 J_0^2/\lambda\sigma T$$

Equations (44) and (45) can be solved analytically in this case, and will be used only when effects of the surface boundary conditions of different physical situations on the discharge instability are examined.

D. Boundary Conditions

The electrical boundary condition on the anode for n_e is given by the following equation, obtained by reasonably assuming the ion flux to be finite across the sheath edge but zero on the surface, from physical considerations of the anode phenomenon.[8]

$$\frac{\epsilon\mu_i}{e}(\nabla\cdot E)E - \frac{\nu}{Sc_i}\left(1 + \frac{T_e}{T}\right)\nabla n_e = -\frac{\mu_i J}{e\mu_e} \tag{46}$$

By substituting Eqs. (12-16) into Eq. (46), the surface boundary condition for n_e is obtained.

The boundary conditions for the steady-state equations, Eqs. (17-20) for the flow and temperature fields are

$$\eta\to\infty: \ f' = 1, \quad \theta = 1, \quad \zeta = 1 \tag{47}$$

$$\eta = 0: \ f = f' = 0, \quad \theta = \theta_w$$

$$A_1(\zeta/\zeta^3) + A_2(1 + \theta_e/\theta)\zeta' = Z \tag{48}$$

where

$$Z = \frac{\mu_i J_0}{e\mu_e n_{e\infty}}\sqrt{\frac{2\xi}{u_\infty\nu}}, \quad \theta_w = \frac{T_w}{T_\infty}$$

As for the boundary conditions for perturbation equations, no perturbation is assumed in the main flow. On the other hand, as the boundary condition on the surface, the following three different kinds of boundary conditions are investigated and the corresponding physical properties of the electrodes are indicated in the parentheses.

$$\eta\to\infty: \quad \hat{t} = \hat{j}_y = \hat{n}_e = 0 \tag{49}$$

$$\eta = 0: \quad Z_1\hat{j}_y + Z_2\hat{n}_e' + Z_3\hat{n}_e + Z_4\hat{t} = 0$$

(i) $\hat{t} = 0$ (thermal-good conductor)

$\hat{j}_y = 0$ (electrical-poor conductor)

(ii) $\hat{t}=0$ (thermal-good conductor)

$\hat{j}_y'=0$ (electrical-good conductor)

(iii) $\hat{t}'=0$ (thermal-poor conductor)

$\hat{j}_y'=0$ (electrical-good conductor) (50)

where

$$Z_1=Z-(2\zeta'/\zeta^3)A_1-(\zeta'/\theta)F_2A_2$$

$$Z_2=-(1/\zeta^3)A_1-(1+\theta_e/\theta)A_2$$

$$Z_3=(3\zeta'/\zeta^4)A_1-(\zeta'/\theta)F_1A_2$$

$$Z_4=(\zeta'\theta_e/\theta^2)A_2-(\zeta'/\theta)F_3A_2$$

The conditions of (i) and (iii) of Eq. (50) are not practical but are expedient in order to investigate effects of low thermal or electrical conductivity on the discharge stability by use of a simplified thin region model previously mentioned.

As the numerical calculation shows, the edge of the boundary layer is almost equivalent to $\eta=4.5$, but perturbed quantities sometimes have nonzero value at this point. It was confirmed from the numerical result that $\eta=8$ is a sufficiently large value to be taken as the outer edge for perturbed terms, and was then put into use in this paper. Among the surface boundary conditions given by Eq. (50), condition (ii) is the most practical for metal electrodes or condensed seed layer on them; therefore, most of the calculations were made on boundary condition (ii). The effect of these respective boundary conditions (i), (ii), and (iii) on the discharge stabililty will be investigated, by use of Eqs. (44) and (45), for the simplified thin region model.

III. Results

A. Case of Electron Thermal and Ionization Nonequilibria

When the current density J_0 under the steady-state condition is given, basic steady-state distributions of unperturbed physical quantities in the anode boundary layer are obtained from Eqs. (17-20) and boundary conditions, Eqs. (47) and (48), and based on this steady, unperturbed distribution, the relation of eigenvalues of h^2 and γ^2 is calculated by Eqs. (34-36) and boundary conditions, Eqs. (49) and (50). The condition (50 (ii)) is used as the surface boundary condition to calculate the eigenvalue of perturbed fields. For h^2 and γ^2, a neutral stability curve for the discharge stability is obtained by carrying out the numerical calculation previously mentioned on the various current densities. The steady, unperturbed hydrodynamical field is characterized by the parameter of x/u_∞, because of the assumption of local similarity as understood from H and R in Eqs. (17-20); therefore, the calculation conditions are selected as $x/u_\infty=1.0\times10^{-3}$s, $T_\infty=2300$ K, and $X_K=0.03\%$. As long as Reynolds number $(=u_\infty x/\nu)$ is less than the critical number of hydrodynamical transition for a laminar flow, this analysis is valid for any pair of x and u_∞ which satisfy the condition previously mentioned (for example, about $x=0.2$ m and $u_\infty=200$ m/s for $Re_x=2\times10^5$). Calculations were made for two cases of surface temperature $T_w=1200$ K and $T_w=700$ K, and effects of surface temperature on the discharge stability were investigated. The neutral stability curves for h^2 and γ^2 thus obtained are shown in Fig. 2, by which it was proven that a transition of discharge mode could be generated as electrothermal instability for small perturbation of a specific wave number. That is, when the parameter h^2, expressed by Eq. (37), is smaller than the critical value, discharge of diffuse mode is stable for small perturbation at any wave number. However, when h^2 exceeds

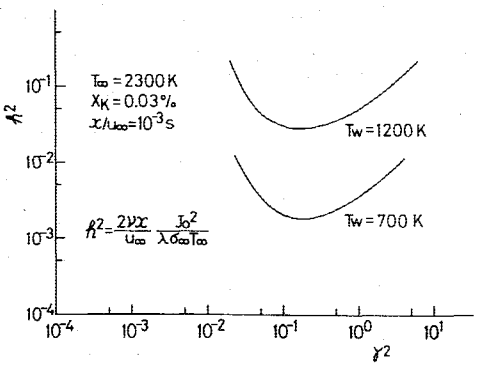

Fig. 2 Neutral stability curves.

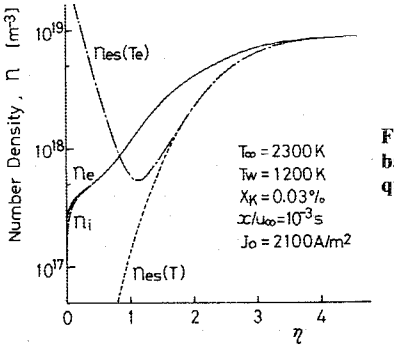

Fig. 3 Distributions of basic and steady physical quantities.

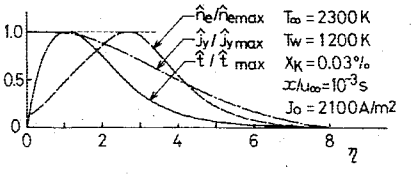

Fig. 4 Distributions of perturbed physical quantities.

this critical value, it is considered that a transition of discharge mode from diffuse to constricted occurs. The current density corresponding to the critical value h_{cr}^2 for $T_w=1200$ K is $J_{cr}=2100$ A/m^2, and for $T_w=700$ K is $J_{cr}=500$ A/m^2. It was made clear from this fact that the decrease of surface temperature remarkably reduces the critical current density that could maintain diffuse mode discharge. Effects of the distance x and the main flow velocity u_∞ on the critical current density can be examined from Eq. (37), and it is found that the larger main flow velocity u_∞ increases the critical current density, while the larger distance x decreases it. The steady-state distribution in the boundary layer and the distribution of perturbed field under the condition of critical point for $T_w=1200$ K are shown in Figs. 3 and 4, respectively. It is seen from Fig. 3 that fairly large electron thermal and ionization nonequilibria exist when the surface temperature is low and the seed fraction is small, as shown in Ref. 8. It is seen from Fig. 4 that the distribution of perturbed field extends into the main flow region outside of the thermal boundary layer.

B. Case of the Electron Number Density in Saha Equilibrium of Gas Temperature

It is assumed that the electron number density is given by Saha equilibrium value for the gas temperature, distributions of electron temperature, and electron number density under the steady-state condition are determined from the gas temperature obtained from Eq. (18), and the relation of eigenvalues of h^2 and γ^2 is calculated from Eqs. (40) and (41) and boundary conditions, Eqs. (49) and (50). Equation (50 (ii)), is used as the surface boundary condition in this case. The neutral stability curves obtained regarding θ_w as parameter are shown in Fig. 5. Figure 5 shows that the critical

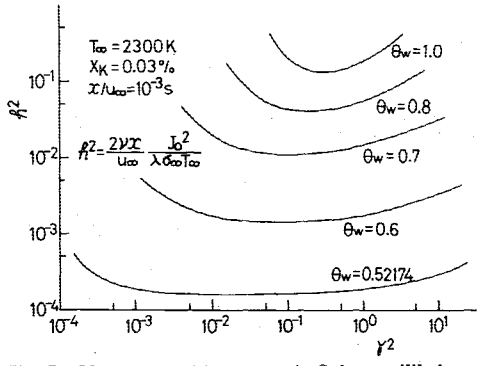

Fig. 5 Neutral stability curves in Saha equilibrium.

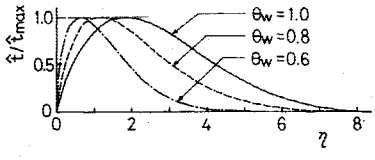

Fig. 6 Distributions of perturbed gas temperature corresponding to Fig. 5.

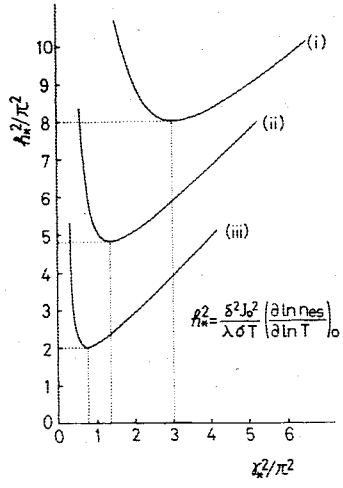

Fig. 7 Effects of surface boundary conditions.

value for the electrothermal instability decreases more rapidly with the surface temperature than in the case of electron thermal and ionization nonequilibria, because in the latter case the electron number density does not decrease as remarkably with the surface temperature, due to the nonequilibrium effect. In Fig. 6, distributions of gas temperature perturbation at respective critical conditions are shown, from which such a characteristic tendency is seen as the region where temperature perturbation exists is getting pushed down to the vicinity of the surface for the low surface temperature. The curve of $\theta_w = 0.52174$ in Fig. 5 is equivalent to that in the case of $T_w = 1200$ K, and comparing this with the critical value in Fig. 2, in the case of $T_w = 1200$ K in electron thermal and ionization nonequilibria, the critical value of the equilibrium case is much lower than that of the nonequilibrium case. It is because of the fact that the low-electrical-conductivity region near the cold surface is the main cause of the discharge instability and that the electron nonequilibrium effect raises the electrical conductivity near the surface.

C. Effect of Surface Boundary Condition

In order to investigate the effect of surface boundary conditions of Eq. (50) on discharge stability, neutral stability cruves for the respective boundary conditions of (i), (ii), and (iii) are calculated by use of a simplified thin region model of Eqs. (44) and (45). The steady-state distribution in this case is assumed uniform in the region of thickness δ. The result obtained is shown in Fig. 7. It is clear from the viewpoint of physical meaning of the respective boundary condition that electrode materials which are good thermal conductors but poor electrical conductors are favorable for the stability of diffuse mode discharge.

IV. Conclusions

A transition of discharge mode from diffuse to constricted in the laminar boundary layer of the seeded combustion gas over a cold anode is analyzed by use of a linear stability theory, and the following conclusions have been obtained.

1) A transition of discharge mode from diffuse to constricted can be generated as electrothermal instability for small perturbations of a specific wave number, when a parameter expressed by a ratio of Joule heat to conductive heat in the gas exceeds a certain critical value.

2) The decrease of surface temperature remarkably reduces the critical current density because the low surface temperature makes the electrical conductivity near the surface low and broadens the low-electrical-conductivity region.

3) The larger main flow velocity increases the critical current density due to a decrease of the thickness of sufficiently low-electrical-conductivity region near a cold electrode. This thickness features the electrothermal instability.

4) When the surface temperature is low and the seed fraction is small, the electrical conductivity near the surface is higher than the equilibrium electrical conductivity for the gas temperature. Therefore, the critical current density is larger than that when the electrical conductivity is assumed in Saha equilibrium for the gas temperature.

5) Although the transition of discharge mode is mainly caused by the low electrical conductivity near the surface of the cold electrode, the perturbed field (particularly the current density perturbation) extends into the main flow region.

6) The stability of diffuse mode discharge is enhanced when one uses electrode materials of high thermal conductivity but low electrical conductivity.

References

[1] Mori, Y., Ohtake, K., and Ogasawara, K., "Experimental Study on Electrical Conductivity of Combustion Gas Plasma and Phenomena near Electrode," 5th International Conference on Magnetohydrodynamic Electrical Power Generation, Munich, 1971, Vol. 1, pp. 11-26.

[2] Dicks, J. B., et al., "The Performance of a Family of Diagonal Conducting Wall MHD Open Cycle Generators," 11th Symposium on Engineering Aspects of Magnetohydrodynamics, Pasadena, Calif., 1970, pp. 16-28.

[3] Messerle, H. K., Campbell, B., and Ho, N. L., "Layer Breakdown on Different Electrode Materials," 6th International Conference on Magnetohydrodynamic Electrical Power Generation, Washington, D.C., 1975, Vol. 1, pp. 389-398.

[4] Hsu, M.S.S., "Thermal Instabilities and Arcs in the MHD Boundary Layers," Paper VI. 6, 13th Symposium on Engineering Aspects of Magnetohydrodynamics, Palo Alto, Calif., 1973.

[5] Oliver, D. A., "Constricted Discharges in Magnetohydrodynamic Plasmas I: A Basic Model," Avco Everett Research Laboratory Report, July 1975.

[6] Oliver, D. A., "A Constricted Discharge in Magnetohydrodynamic Plasma," Paper IX. 4, 15th Symposium on Engineering Aspects of MHD, Philadelphia, Pa., 1976.

[7] Kon, T., Kayukawa, N., Ozawa, Y., and Aoki, Y., "Electrical and Thermal Instabilities in the Electrode Surface Region in a Combustion MHD Generator Channel," Paper VI. 1, 16th Symposium on Engineering Aspects of Magnetohydrodynamics, Pittsburgh, Pa., 1977.

[8] Okazaki, K., Mori, Y., Ohtake, K., and Hijikata, K., "Boundary Layer Analysis of Seeded Combustion Gas Near a Cold Electrode," *AIAA Journal*, Vol. 15, Dec. 1977, pp. 1778-1784.